

Ab initio calculation of the reflectance anisotropy of GaAs(110)

Olivia Pulci, Giovanni Onida, and Rodolfo Del Sole

*Istituto Nazionale per la Fisica della Materia, Dipartimento di Fisica dell' Università di Roma Tor Vergata,
Via della Ricerca Scientifica, I-00133 Roma, Italy*

Anatoli J. Shkrebtii

Department of Physics, University of Toronto, 60 St. George Street, Toronto, Ontario, Canada M5S 1A7

(Received 17 June 1997; revised manuscript received 12 December 1997)

We compute the optical properties of the (110) surface of gallium arsenide within the first-principles density-functional theory local-density approximation scheme, using norm-conserving pseudopotentials. Starting from the surface electronic structure calculation, we analyze the imaginary part of the theoretical dielectric function, separating surface and bulk contributions. The effects of the nonlocality of the pseudopotential are studied, by working both in the transverse gauge (neglecting them) and in the longitudinal gauge (where they are automatically included). The two calculations, although giving different dielectric functions, yield the same reflectance anisotropy, which compares well with experimental data and with previous theoretical results. [S0163-1829(98)02228-0]

I. INTRODUCTION

In the last years, the atomic geometry and electronic properties of the GaAs(110) surface have been successfully determined, both from the experimental and theoretical points of view (see Ref. 1 and references therein). Its surface optical spectra are more difficult to interpret, because optical transitions involving surface states overlap the energy range of the corresponding bulk transitions. There is then a strong need for sufficiently accurate calculations of the spectra provided by reflectance anisotropy spectroscopy (RAS) and surface differential reflectivity.

The present state of the art of the calculations of surface optical properties is the semiempirical tight-binding method, whose results are usually in fair agreement with experiments.² However, it would be desirable to carry out calculations of surface optical properties based on a self-consistently determined electronic structure. Some steps in this direction have already been taken. A self-consistent plane-wave calculation of GaAs and GaP(110) optical properties was carried out by Manghi *et al.*, using local pseudopotentials and the X_α scheme to account for the exchange-correlation potential.³ Very recently, *ab initio* calculations using non-local norm-conserving pseudopotentials within a strict density-functional theory (DFT) framework have appeared for GaAs(100),⁴ Si(100),^{5,6} and C(100) surfaces.⁶ Their results for the reflectance anisotropy (RA) are not completely satisfactory, being sometimes at variance with experiments [in the case of GaAs(100)], and sometimes at variance with physical expectation [in the case of Si(100) 2×1].

It is not yet clear whether DFT-LDA (local-density-approximation) wave functions are precise enough to yield good oscillator strengths and meaningful surface optical spectra, which need, in principle, quasiparticle wave functions and energies, e.g., calculated according to the so-called *GW* approximation, and consideration of electron-hole interaction effects. In order to check this point, it is worthwhile to carry out well-converged DFT-LDA calculations for many

surfaces, to be compared with experiments and with *GW* calculations, when these will be available.

Here we present a first-principles calculation of the optical properties of GaAs(110), using state-of-the-art DFT in the LDA, and norm-conserving *ab initio* pseudopotentials. It is well known that the usual formulation of the interaction of light with matter, based on the $\mathbf{A} \cdot \mathbf{p}$ formulation within the transverse gauge, cannot be applied in the presence of a non-local pseudopotential, V_{NL} . That is, \vec{p} should be replaced by $\vec{p} + i[V_{NL}, \vec{r}]$, following, e.g., the procedure given in Appendix B of Ref. 7. Another possibility, which in this case turns out to be numerically more convenient, is to work within the so-called longitudinal gauge, in which the long-wavelength radiation is described as a scalar field. In this scheme, the formulation remains the same for local and nonlocal potentials.⁸ In order to check the importance of this point in the case of surfaces, we carry out calculations of optical properties, both neglecting and including the pseudopotential nonlocality effects. Although the two calculations yield slightly different results for bulk semiconductors, quite surprisingly we find that the relative surface contribution to reflectance comes out nearly identical in the two approaches, up to 5 eV.

We compare our results with reflectance anisotropy data^{9,10} and with previous^{3,10,11} calculations. We obtain a RA line shape in fairly good agreement with experiments and with previous theoretical results.¹⁰

II. THEORY

A. Surface optical properties

Accounting for the nonlocality, anisotropy, and inhomogeneity of the surface dielectric tensor, the correction to Fresnel's formulas for the reflectivity for normally incident light is given by¹²

$$\frac{\Delta R_\alpha(\omega)}{R_0(\omega)} = \frac{4\omega}{c} \text{Im} \frac{\Delta \epsilon_{\alpha\alpha}(\omega)}{\epsilon_b - 1}, \quad (1)$$

where ϵ_b is the bulk dielectric function, R_0 is the standard Fresnel reflectivity, and the subscript α refers to the direction of light polarization. The reflectance anisotropy spectrum, defined as

$$\frac{\Delta R}{R} = \frac{\Delta R_y(\omega) - \Delta R_x(\omega)}{R_0(\omega)}, \quad (2)$$

can then be computed in term of the quantity $\Delta\epsilon_{\alpha\alpha}(\omega)$, which is directly related to the macroscopic dielectric tensor $\epsilon_{\alpha\beta}$ of a semi-infinite solid,¹³ and is dimensionally a length.

In a repeated-slab geometry, introduced in order to simulate the real surface, $\Delta\epsilon$ is given by³

$$\Delta\epsilon_{\alpha\alpha}(\omega) = d[1 + 4\pi\alpha_{\alpha\alpha}^{hs}(\omega) - \epsilon_b(\omega)], \quad (3)$$

where d is half of the slab thickness and $\alpha_{\alpha\alpha}^{hs}(\omega)$ is the polarizability of a half-slab. For this geometry, the change of reflectivity with respect to the Fresnel formulas then reduces to

$$\frac{\Delta R_\alpha(\omega)}{R_0(\omega)} = \frac{4\omega d}{c} \text{Im} \frac{4\pi\alpha_{\alpha\alpha}^{hs}(\omega)}{\epsilon_b - 1}. \quad (4)$$

In the single particle scheme, the imaginary part of α^{hs} takes the standard expression

$$\alpha_{\alpha\alpha}^{hs(2)}(\omega) = \frac{\pi e^2}{m^2 \omega^2 A d} \sum_{\mathbf{k}, v, c} |p_{vc}^\alpha(\mathbf{k})|^2 \delta[E_c(\mathbf{k}) - E_v(\mathbf{k}) - \hbar\omega] \quad (5)$$

involving the transition probability between slab valence and conduction bands, of energy $E_v(\mathbf{k})$ and $E_c(\mathbf{k})$ respectively; $p_{vc}^\alpha(\mathbf{k})$ is the matrix element of the momentum operator, and A is the area of the sample surface.

Using the momentum operator $\vec{p} = (\hbar/i)\vec{\nabla}$ within the transverse gauge to describe the coupling of electrons with the radiation is equivalent to ignoring the contributions from the nonlocal part of the pseudopotential, V_{NL} . These contributions can be included either replacing \vec{p} with $\vec{p} + i[V_{NL}, \vec{r}]$,⁷ or working within the longitudinal gauge, where the perturbing operator is $e^{i\mathbf{q}\cdot\mathbf{r}}$, with \mathbf{q} vanishingly small.^{8,14}

$$\alpha_{\alpha\alpha}^{hs(2)}(\omega) = \frac{\pi e^2}{A d} \lim_{q \rightarrow 0} \frac{1}{q^2} \sum_{v, c} \sum_{\mathbf{k}} | \langle v, \mathbf{k} + q\hat{\mathbf{e}}_\alpha | e^{i\mathbf{q}\cdot\mathbf{r}} | c, \mathbf{k} \rangle |^2 \times \delta[E_c(\mathbf{k}) - E_v(\mathbf{k}) - \hbar\omega]. \quad (6)$$

This leads, however, to calculating the wave functions at four grids of \vec{k} points, namely, at \vec{k} and $\vec{k} + q\hat{\mathbf{e}}_\alpha$ ($\hat{\mathbf{e}}_\alpha$ is the unit vector directed along the α axis), multiplying by 4 the already heavy computational work. We have used both approaches in calculating the optical properties of bulk GaAs, not including, however, the commutator $[V_{NL}, \vec{r}]$ in the transverse gauge. Hence, the difference between the two approaches is an indication of the size of pseudopotential-nonlocality effects on the optical properties. Differences of about 10% are obtained in bulk GaAs.¹⁴ Since in the case of the surface we look at effects of the order of 1%, it is important to take the nonlocality of the pseudopotential into account. In order to check this point, which had been over-

looked in previous *ab initio* calculations,⁴⁻⁶ we have calculated the surface optical properties of GaAs(110) using both methods.

B. Electronic structure

Our calculation of the optical response of the GaAs(110) surface starts with the computation of the single-particle spectrum and the transition probability between occupied and unoccupied states, for both the bulk and slab geometries. We compute the band structure and the momentum matrix elements within the standard DFT-LDA scheme,¹⁵ using a plane-waves basis set, and the Ceperley-Alder¹⁶ LDA exchange-correlation potential as parametrized by Perdew and Zunger.¹⁷ The use of norm-conserving, hard-core,¹⁸ fully separable pseudopotentials of the Bachelet-Hamann-Schlüter type^{19,20} ensures good transferability properties.

We describe the GaAs(110) surface using a repeated slab made of 11 atomic layers plus seven empty layers, in order to minimize the spurious interactions between different surfaces. A check, carried out with 13+7 layers, has shown that good convergence has been achieved. The atomic positions correspond to a fully relaxed configuration, obtained by a Car-Parrinello molecular-dynamics run.²¹ Once the ground-state charge density has been determined, the true filled and empty Kohn-Sham (KS) eigenfunctions are determined by a full diagonalization of the KS Hamiltonian. This technical point, that is irrelevant when only the total energy and the total charge density are of interest, becomes important when individual state wave functions are needed.²² An energy cutoff of 15 Ry was chosen, which ensures a convergence of the eigenvalues within 50 meV.

The convergence with respect to the \vec{k} -point sampling, which represents one of the major bottlenecks in optical properties calculations, has been carefully tested. For the bulk calculations, a well-converged 825 special points set in the irreducible wedge of the Brillouin zone (BZ) has been used. In the case of the slab, we have checked convergence of the calculated RA using 16, 36, 64, and 100 two-dimensional \vec{k} points in the irreducible wedge of the surface BZ [see Fig. 1(a)]. The 64 special-point set appears to be sufficient to obtain qualitatively stable results, with low-energy structures (0–5 eV) converging faster than the higher part of the spectra. From the differences appearing in Fig. 1(a), and from independent tight-binding calculations carried out with 1024 \vec{k} points,²³ we estimate that the RA structures at full convergence might be still reduced with respect to the present results.

The convergence with respect to the slab thickness has also been checked, by performing the RA calculation for 11- and 13-layer slabs, using the same set of 64 \vec{k} points [see Fig. 1(b)]. The energy positions of the RA structures are unchanged, with small differences (about 10%) in the peak intensities.

III. RESULTS

A. Bulk results

Our results for the GaAs bulk dielectric function are discussed in Ref. 14. A direct minimum gap of 1.37 eV has

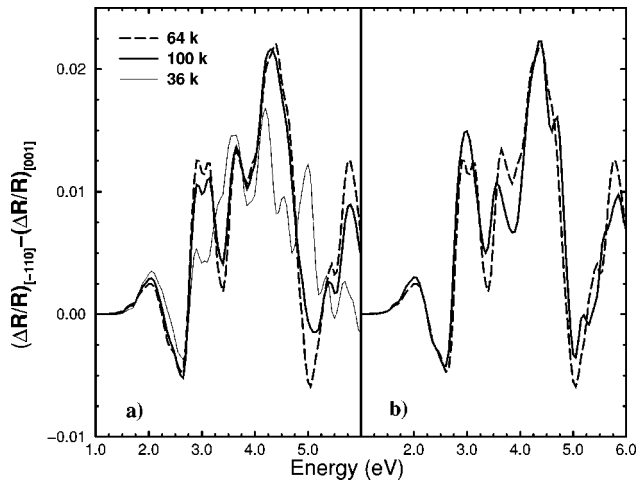


FIG. 1. Convergence tests of the reflectance anisotropy: (a) with respect to the number of \vec{k} points used to sample the irreducible part of the Brillouin zone (the result obtained with 16 \vec{k} points is not shown, because it is very far from being converged); and (b) with respect to the thickness of the slab: results for 11 (dashed line) and 13 (solid line) atomic layers.

been obtained, quite a bit larger than the values quoted in the literature for well-converged LDA calculations at the experimental lattice constant. This is a consequence of using the calculated lattice constant, which is 1.5% smaller than the experimental one, and neglecting nonlinear core corrections,²⁴ as discussed in Ref. 14. The higher gaps are less sensitive to these details, so that they are in good agreement with the values usually quoted in the literature. Because of the gap problem of DFT-LDA, they are about 0.8 eV smaller than the experimental values determined from direct and inverse photoemission. Since optical transitions are rather weak at the fundamental gap and stronger at the higher gaps, we believe that the large value of the direct gap found in our calculation will not qualitatively affect the calculated spectra.²⁵ As expected, a direct comparison with the experimental data of Ref. 26 shows a satisfactory, although not perfect, agreement. In fact, the direct interpretation of the Kohn-Sham eigenvalues of the DFT-LDA as excitation energies is in general not correct:²⁷ in principle, one should compute the true quasiparticle energies and also, in the case of absorption spectra, include excitonic effects. The computed main structures of our LDA ϵ_b are similar to the previous X_α results by Manghi *et al.*³ for the same system.

B. Surface calculations

Our results for the surface band structure are given in Fig. 2. Surface states have been identified computing the localization of the squared modulus of the wave functions in the surface region. We identify several surface bands (full dots in Fig. 2), corresponding to the C_1 - C_4 and A_1 - A_5 bands of Ref. 3.

As in Ref. 3, the As bands lying at the top of the valence band show little dispersion. By contrast, the first unoccupied surface band (Ga type) displays a rather large dispersion (~ 1.3 eV), and along the XM direction it separates from the projected bulk continuum by about 0.7 eV. As a consequence

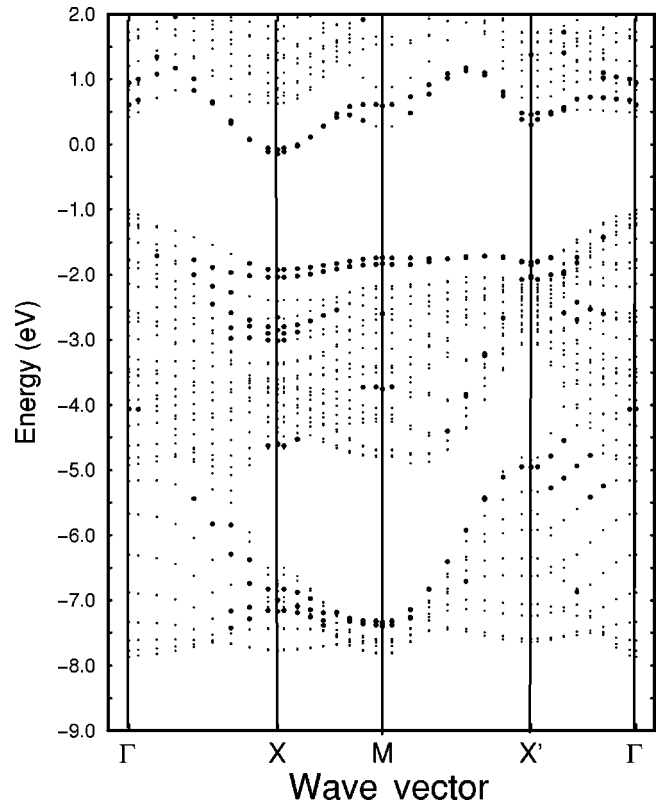


FIG. 2. Computed surface band structure of GaAs(110). Full dots are used for states localized at the surface. These are defined as those states whose squared modulus integrated over the two outermost layers exceeds 0.275 (this is about 50% more than for a state equally distributed over all layers, whose localization on the outermost two layers is $2/11=0.18$).

of the relatively large bulk gap found in our calculation, this surface state at X is well within the forbidden gap, in contradiction with experimental data on Fermi-level pinning.²⁸ This shortcoming, which is common to calculations using the Kleinman-Bylander form of the present pseudopotential at the theoretical lattice constant, and neglecting nonlinear core corrections,¹ is due to the aforementioned inaccuracy in the determination of the fundamental bulk gap, while our surface-state band structure is in good agreement with experiments,^{29,30} once a quasiparticle upward shift of about 0.8 eV is applied to the empty bands.³¹ On the other hand, the rather large separation of the lowest unoccupied surface band from the continuum of (slab) conduction bands at X, about 0.8 eV, is an artifact due to the size quantization of bulk states in the slab.³² Actually, the separation of this state from the projected bulk band structure at X is only ≈ 0.4 eV, in agreement with other calculations.³³

The diagonal components of the imaginary part of the half-slab polarizability $\alpha_{\alpha\alpha}^{hs}(\omega)$ (multiplied by $4\pi d$), computed in both the transverse (T) and longitudinal (L) gauges, according to Eqs. (5) and (6), respectively, are shown in Fig. 3. Results for light polarization along x (the electric field in the direction $[001]$, that is perpendicular to the atomic chains) and y (the electric field parallel to the chains, direction $[\bar{1}10]$) are reported in Figs. 3(a) and 3(b), respectively. As in the case of the bulk spectrum, the L -gauge result is slightly larger than that of the T gauge, for both polariza-

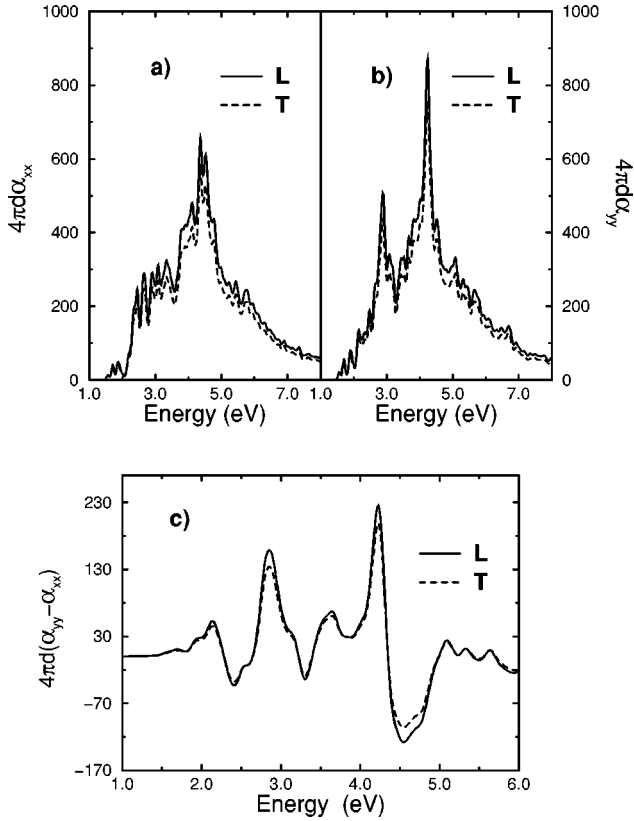


FIG. 3. Diagonal components, in the surface plane, of the imaginary part of the half-slab polarizability calculated neglecting [T , according to Eq. (5)] or taking into account [L , according to Eq. (6)] the nonlocality of the pseudopotentials. (a) Light polarization perpendicular to the chain direction. (b) Light polarization parallel to the chains. (c) The difference between (b) and (a).

tions. The difference of the x and y polarizabilities, shown in Fig. 3(c), is also slightly larger in absolute value for the L gauge.

The main features of xx and yy spectra are similar; however, there are important differences due to the anisotropy of the surface. These differences come into evidence in the reflectance anisotropy spectrum [Fig. 4(a)], which we have computed according to Eq. (2). Quite surprisingly, the RA for the two gauges is nearly identical up to 6 eV. The same is true for the surface contributions to reflectance, calculated according to Eq. (1), separately for x and y polarizations. The reason is that the bulk dielectric function, which appears in the denominator of Eq. (1) and (2), is also affected by the choice of the gauge (see Ref. 14). Although the transverse-gauge formula (5) does not correctly account for the pseudopotential non-locality, the effects of the latter on the spectra is a slight scaling up, by the same factor for bulk, slab x and slab y polarizations. When ratios between polarizabilities are calculated, as in Eqs. (1) and (2), the common factor disappears, and the RA results are not affected by the pseudopotential nonlocality.

We are interested in the range of frequencies below 5 eV, for which experimental RAS data are available, and the calculated spectra are well converged with respect to the sums over empty states. In this range the theoretical RAS spectrum [Fig. 4(a)] shows a positive peak S at ≈ 2.0 eV, becomes

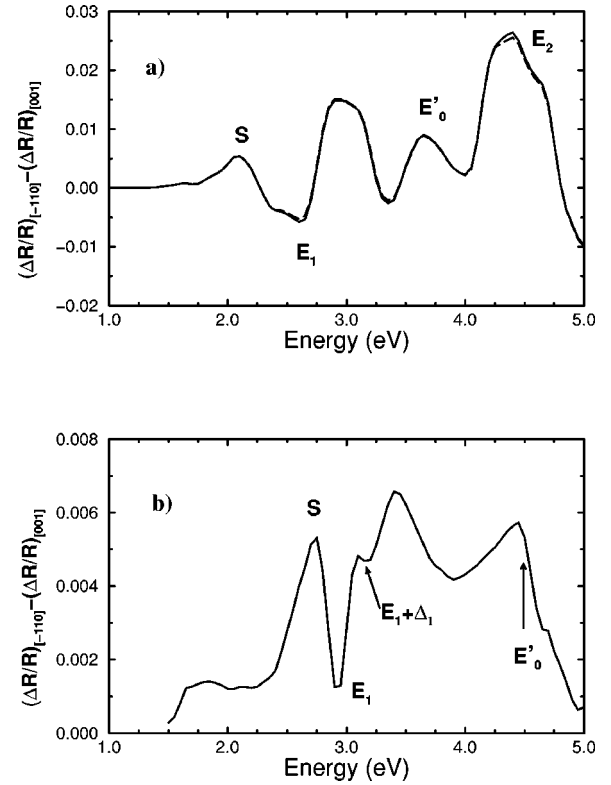


FIG. 4. (a) Reflectance anisotropy spectrum of GaAs(110) computed according to Eqs. (5) and (6) (T and L , respectively) for an 11-layer slab. The two curves are almost indistinguishable up to 6 eV. (b) Measured reflectance anisotropy for GaAs(110), from Ref. 10.

negative around ≈ 2.7 eV, and displays positive structures near 3.0, 3.7, and 4.4 eV. We show in Fig. 4(b) the room-temperature experimental data of Esser *et al.*¹⁰ A previous experiment was carried out in Ref. 9 at low temperature in a narrower frequency range. Here we show the spectrum taken at room temperature, because of its more extended frequency range. The two experimental spectra are consistent each other, if we accept that a considerable broadening is present at room temperature.¹¹ As a consequence, the two peaks S_1 and S_2 and the shoulder at 2.95 eV of the low- T spectrum of Ref. 9 coalesce altogether in the broad structure S , centered at 2.8 eV in the room-temperature spectrum. This structure corresponds to the calculated one centered around 2 eV, which is mostly due to transitions from the highest filled to the lowest empty surface state band shown in Fig. 2. The shift is of course due to the gap problem of DFT-LDA. Less accurate results, which have been presented previously,³⁴ are used for the convergence tests shown in Figs. 1(a) and 1(b); here the 2-eV peak is about twice as weak as in Fig. 4(a), and the agreement with experiment is hence worse. Improvements in the convergence of the dynamical algorithm yielding the wave functions has lead to the results of Fig. 4(a), which better compare with experiment and previous calculations. The higher intensity and narrow width of the S_1 peak in the experiment of Ref. 9 is probably a consequence of the occurrence of excitonic effects at low temperatures.

The other calculated structures are also in agreement with experiment. They are all due to transitions between surface

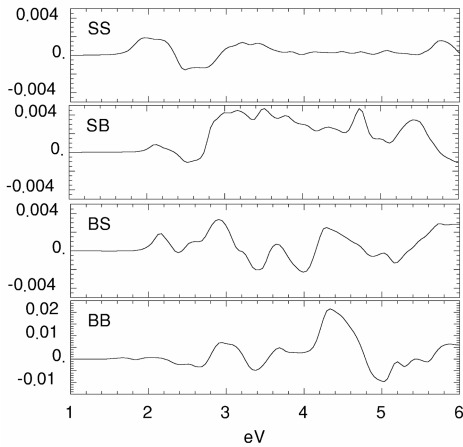


FIG. 5. Decomposition of the RAS spectrum into surface-surface (ss), surface-bulk (sb), bulk-surface (bs), and bulk-bulk (bb) contributions to the reflectance anisotropy spectrum (see text).

perturbed bulk states, as it will be shown below. The RA dip at 2.6 eV (which, together with the subsequent peak at ~ 3 eV, is due to the bulk E_1 structure) corresponds to the experimental dip near 3 eV; the calculated peak at 3 eV, and the structure at 3.7 eV related to the E'_0 bulk structure, correspond well to the experimental structures at 3.4 and 4.5 eV, respectively. The weak dip at about 3.1 eV in Fig. 4(b), due to the $E_1 + \Delta_1$ transition, is not present in our calculation because we neglect spin-orbit interaction. The calculated peak at 4.4 eV is due to the E_2 structure, which occurs above 5 eV in the bulk experimental spectrum. The overestimation of the RAS structures different from S is probably due, in addition to electron-hole interaction effects, also to the aforementioned problem of the \vec{k} -point summation: in tight-binding calculations, indeed, the intensities of these structures decrease by a factor of about 2 going from 64 \vec{k} points to full convergence (1024 \vec{k} points).²³

In order to analyze the nature of the RAS structures, we have decomposed the spectrum, by separating the optical transition between bulk states (bb), from bulk to surface states (bs), from surface to bulk states (sb), and between surface states (ss). The results for the partial spectra are reported in Fig. 5. From this analysis, it appears that the first peak S (around 2 eV) has, as anticipated before, a substantial ss character, while most of the structures between 3 and 4.5 eV are due to bb transitions, with small bs and sb contributions. These results make the comparison of our RAS results with previous pseudopotential X_α calculations by Manghi *et al.*³ not straightforward. In fact, apart from the energy shift, which could be expected since we use standard LDA, our S peak is mainly due to surface-surface transitions along the X - M direction, while in the X_α calculation the first peak is due to bulk-bulk transitions, and located at about 2.6 eV.

In Ref. 3, the experimental $S1$ and $S2$ peaks were recognized as their peaks labeled $F1$ and $F2$, and it was concluded that the main contribution to reflectance anisotropy comes from bulk-bulk transitions. In the present LDA scheme, surface-surface contributions are present at the lowest energies, while bb transitions become important above 2.5 eV.

The ss contributions involve the first empty surface band, which, at variance with Ref. 3, is well separated from the bulk conduction band, entering deeply into the gap near the X point. This discrepancy in band positions is the reason of the different interpretations of the ss contributions in this work and in Ref. 3.

A last point to be remarked is that the shifts between the calculated RA structures and the experimental ones is larger for the ss-related structure (about 0.8 eV) than for bb-related structures (about 0.4 eV). Such shifts are due to the quasiparticle corrections to DFT-LDA, which tend to increase the transition energies, partially reduced by the electron-hole interaction, which decreases transition energies. The difference mentioned above between surface-state-related and bulk-state-related shifts suggests that quasiparticle shifts are larger at this surface than in bulk GaAs, as it was previously argued in Ref. 35.

IV. CONCLUSIONS AND FUTURE WORK

We have presented a DFT-LDA calculation of the surface optical anisotropy of the GaAs(110) surface. The agreement with RAS experiments is fairly good. The first RA peak on the low-frequency side embodies a substantial contribution of transitions between surface states, while the higher-energy features are mostly due to transitions between surface perturbed bulk states.

We have found that a high numerical accuracy and convergence in all computational ingredients is necessary to obtain reproducible results, in particular when the low-frequency ss-related peak is concerned. We emphasize the need of many \vec{k} points to obtain well-converged spectra within the DFT-LDA pseudopotential approach. This result leads us to question the reliability of *ab initio* calculations of surface optical properties carried out using a small number of \vec{k} points. On the other hand, considering or not considering the nonlocality of the pseudopotential does not affect the surface contribution to reflectance. This is an important point for future calculations of surface optical properties, which can be carried out within the computationally less demanding transverse gauge.

It is well known that the use of the DFT-LDA eigenvalues to interpret directly the absorption spectra is an oversimplification. Nevertheless, it has been found that this approach is able to give quite satisfactory results for bulk semiconductors.^{14,36} The present work suggests that the same is true in the case of GaAs(110).

ACKNOWLEDGMENTS

We acknowledge useful discussions with Friedhelm Bechstedt, Clemens Kress, and Rita Magri. We are grateful to Matthias Scheffler for providing us with the CARPARRINELLO computer code, which has been used in part of the present work. This work was supported in part by the European Community program ‘‘Human Capital and Mobility’’ through Contract No. ERB CHRX CT930337. Computer resources on the Cray C92 and parallel Cray T3D were granted by CINECA (Interuniversity Consortium of North-eastern Italy for Automatic Computing) (Grant Nos. 96/94-5 and 96/101-5, and INFN account cmprmp0).

- ¹J. L. A. Alves, J. Hebenstreit, and M. Sheffler, *Phys. Rev. B* **44**, 6188 (1991).
- ²R. Del Sole, in *Photonic Probes of Surfaces*, edited by P. Halevi (Elsevier, Amsterdam 1995), p. 131.
- ³F. Manghi, R. Del Sole, A. Selloni, and E. Molinari, *Phys. Rev. B* **41**, 9935 (1990).
- ⁴S. J. Morris, J. M. Bass, C. C. Matthai, V. Milman, and M. C. Payne, *J. Vac. Sci. Technol. B* **12**, 2684 (1994); S. J. Morris, J. M. Bass, and C. C. Matthai, *Phys. Rev. B* **52**, 16 739 (1995).
- ⁵L. Kipp, D. K. Biegelsen, J. E. Northrup, L.-E. Swartz, and R. D. Bringans, *Phys. Rev. Lett.* **76**, 2810 (1996).
- ⁶C. Kress, A. I. Shkrebtii, and R. Del Sole, *Surf. Sci.* **377-79**, 398 (1997).
- ⁷M. S. Hybertsen and S. G. Louie, *Phys. Rev. B* **35**, 5585 (1987).
- ⁸A. F. Starace, *Phys. Rev. A* **3**, 1242 (1971).
- ⁹V. L. Berkovits, V. A. Kiselev, and V. I. Safarov, *Surf. Sci.* **211/212**, 489 (1989).
- ¹⁰N. Esser, N. Hunger, J. Rumberg, W. Richter, R. Del Sole, and A. I. Shkrebtii, *Surf. Sci.* **307/309**, A 1045 (1994).
- ¹¹A. I. Shkrebtii and R. Del Sole (unpublished).
- ¹²A. Bagchi, R. G. Barrera, and A. K. Rajagopal, *Phys. Rev. B* **20**, 4824 (1979); R. Del Sole, *Solid State Commun.* **37**, 537 (1981).
- ¹³R. Del Sole and E. Fiorino, *Phys. Rev. B* **29**, 4631 (1984).
- ¹⁴O. Pulci, G. Onida, A. I. Shkrebtii, R. Del Sole, and B. Adolph, *Phys. Rev. B* **55**, 6685 (1997).
- ¹⁵R. M. Dreizler and E. K. U. Gross, *Density Functional Theory* (Springer, Berlin, 1990).
- ¹⁶D. M. Ceperley and B. J. Alder, *Phys. Rev. Lett.* **45**, 566 (1980).
- ¹⁷J. P. Perdew and A. Zunger, *Phys. Rev. B* **23**, 5048 (1981).
- ¹⁸By “hard core,” we mean choosing a conservatively small value for the pseudopotential radius r_c , beyond which the pseudo-wave-function and all-electron wavefunction coincide. Larger values of r_c generally produce “softer” pseudopotentials, which require a smaller energy cutoff to converge, but whose transferability can be worse.
- ¹⁹G. Bachelet, D. R. Hamann, and M. Schlüter, *Phys. Rev. B* **26**, 4199 (1982).
- ²⁰L. Kleinman and D. M. Bylander, *Phys. Rev. Lett.* **48**, 1425 (1982).
- ²¹G. Schmidt, F. Bechstedt, and G. P. Srivastava, *Phys. Rev. B* **52**, 2001 (1995).
- ²²In fact, when the energy functional of DFT is minimized via a dynamical algorithm, avoiding the explicit diagonalization of the Kohn-Sham Hamiltonian, as we do in the Car-Parrinello method, the resulting set of one-particle states Ψ 's is only guaranteed to give the right total charge and sum of diagonal H matrix elements, and hence the right total energy, but they do not necessarily coincide with H eigenvectors. Instead, the Ψ 's are related to the eigenvectors via an arbitrary unitary transformation in the full subspace of the occupied states. Another important technical point is that, in order to obtain the RA, which is of the order of 1% of the reflectance, with reasonable accuracy, one must employ very accurate wave functions to determine the optical matrix elements. Hence the convergence of the algorithm leading to the wave functions is crucially important. The curves shown in Figs. 3, 4, and 5 have been obtained using the fully converged wave functions. On the other hand, the convergence tests shown in Figs. 1(a) and 1(b) have been done using less accurate wave functions.
- ²³G. Onida and R. Del Sole (unpublished).
- ²⁴S. G. Louie, S. Froyen, and M. L. Cohen, *Phys. Rev. B* **26**, 1738 (1982).
- ²⁵The relatively high value of the gap at Γ is a common feature of the calculations, which employ the present pseudopotential at the theoretical lattice constant. We have repeated the calculations using a different numerical pseudopotential generated within the Hamann scheme [D. R. Hamann, *Phys. Rev. B* **40**, 2980 (1989)], yielding a smaller direct bulk gap of 0.8 eV. Nevertheless, the RA spectra calculated using the two pseudopotentials are very similar to each other. This substantiates our conjecture that the value of the minimum bulk gap is not important for obtaining the surface optical properties. As a consequence, the inclusion of nonlinear core corrections, whose main effect is to reduce the bulk minimum gap, is not expected to change qualitatively the present results.
- ²⁶D. E. Aspnes and A. A. Studna, *Phys. Rev. B* **27**, 985 (1983).
- ²⁷R. W. Godby, M. Schlüter, and L. J. Sham, *Phys. Rev. B* **37**, 10 159 (1988).
- ²⁸A. Huijser, J. van Laar, and T. L. van Rooy, *Surf. Sci.* **62**, 472 (1977).
- ²⁹D. Straub, M. Skibowski, and F. Himpsel, *Phys. Rev. B* **32**, 5237 (1985); M. Skibowski and L. Kipp, *J. Electron Spectrosc. Relat. Phenom.* **68**, 77 (1994).
- ³⁰H. Carstensen, R. Claessen, R. Manzke, and M. Skibowski, *Phys. Rev. B* **41**, 9880 (1990).
- ³¹Actually a larger shift should be applied to the empty surface bands to agree with the findings of B. Reihl, T. Riesterer, M. Tschudy, and P. Perfetti, *Phys. Rev. B* **38**, 13 456 (1988). In this work, however, the gaps between surface states are larger than those of Ref. 30.
- ³²A typical energy of size quantization effects is $E_{SQ} = \hbar^2(\pi/L)^2/2m^*$, where L is the slab thickness and m^* the relevant effective mass. Taking a slab of 11 (110) layers and $m^* = 0.1m_e$, we obtain $E_{SQ} = 0.8$ eV, which is of the right order of magnitude to account for the discrepancy between the bulk-projected and slab values of the conduction-band edge at X .
- ³³X. Zhu, S. B. Zhang, S. G. Louie, and M. L. Cohen, *Phys. Rev. Lett.* **63**, 2112 (1989).
- ³⁴O. Pulci, G. Onida, C. Kress, A. I. Shkrebtii, and R. Del Sole, in *Proceedings of the 23rd International Conference on the Physics of Semiconductors, Berlin, 1996*, edited by M. Sheffler and R. Zimmerman (World Scientific, Singapore, 1996), p. 815.
- ³⁵F. Bechstedt, R. Del Sole, and F. Manghi, *J. Phys. (Paris)* **1**, SB75 (1989); F. Bechstedt and R. Del Sole, *Solid State Commun.* **74**, 41 (1990).
- ³⁶B. Adolph, V. Gavrilenko, K. Tenelsen, F. Bechstedt, and R. Del Sole, *Phys. Rev. B* **53**, 9797 (1996).